THE JOURNAL OF PHYSICAL CHEMISTRY C

ARTICLE

pubs.acs.org/JPCC

Correlation between Annealing-Induced Growth of Nanocrystals and the Performance of Polymer: Nanocrystals Hybrid Solar Cells

Weili Yu, Hao Zhang, Hongru Tian, Haotong Wei, Wenxu Liu, Jian Zhu, Junhu Zhang, and Bai Yang*

State Key Lab of Supramolecular Structure and Materials, College of Chemistry, Jilin University, Changchun 130012, People's Republic of China

Supporting Information

ABSTRACT: In this work, we investigated the correlation between the inner structure of aqueous solution processed polymer:nanocrystals (NCs) hybrid solar cells and its performance. By altering the compositional concentration, annealing temperature, annealing time, and the thickness of the active layer, the diameter of CdTe NCs increased from 2.8 nm to tens of nanometers. Also, the performance of poly (1,4-phenylene vinylene) (PPV):CdTe hybrid solar cells changed accordingly. Systematical analysis revealed that the best performance of hybrid solar cells was achieved when CdTe was 30 mg/mL and the annealing temperature was above 250 °C with the active layer thickness of about 100 nm. The inner structure showed the size of CdTe NCs was around 26 nm, with the spacing of 6−12 nm. The data of transmission electron microscopy (TEM) and X-ray diffraction (XRD) confirmed that the CdTe NCs grew mainly via dynamic coalescence.

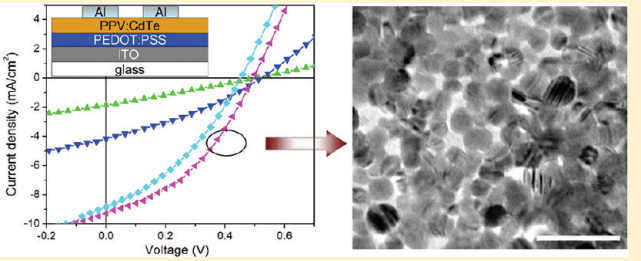

INTRODUCTION

Solution-processed films employing polymer and semiconductor nanocrystals (NCs) offer the potential to produce large area, low-cost, and flexible solar cells with high efficiencies.[1−3] Continuous progress in improving the power conversion efficiency (PCE) has been achieved by introducing flexible conjugated polymers and NCs with higher carrier mobility. Up to now, typical polymer materials include the derivates of polythiophene, for example, poly(3-hexylthiophene) (P3HT),[1] or different types of poly (1,4-phenylene vinylene) (PPV) derivatives, for example, poly[2-methoxy-5-(3,7-dimethyloctyl oxy)]-1,4-phenylenevinylene (MDMO-PPV),[4] etc. The widely investigated NCs include TiO_2,[5] ZnO,[6] CdSe,[1] PbS,[7] PbSe,[8] etc. Although some progress has been made in this area, two environmental obstacles still need to be overcome before a fully green-fabricated solar cell was realized, that is, the liquid/air pollution caused by the organic solvents and energy consumed during material synthesis and device fabrication. In particular, the widely used polymers and inorganic colloidal NCs are synthesized and dissolved in organic solvents, such as chloroform, benzene, chlorobenzene, etc. The toxicity and flammability are crucial for the people working at the manufacturing machine. The cumulative energy needed for raw materials production will severely extend the energy payback time of the solar cells.[9]

In recent years, water-soluble materials have attracted considerable attention because they are green and environmentally friendly. Moreover, life cycle analysis has shown that water has much lower embedded energy than do organic solvents.[10,11] In this field, recently we have demonstrated an efficient polymer/NCs hybrid solar cell with the donor material of PPV and acceptor material of CdTe NCs.[12] According to this work, the device fabrication could be conducted in air, thus relieving liquid/air pollution, as well as the energy consumed. Following this research, feasible materials for processing solar cells are expected to extend to more water-soluble materials, such as polyelectrolytes, NCs, and semiconductor materials with nonionic alcohol or glycol side chains.[9]

Although a simple annealing process has been proved effective in changing an insulator hybrid film into light active layer, the correlationship between inner structure of hybrid film and performance of hybrid solar cell is still not fully understood, neither is the effect of the evolution of NCs on device performance during the annealing process. The annealing-induced transition from PPV precursor to PPV has been widely investigated,[13,14] which elucidates the mechanism of the elimination reaction,[15] as well as the effect of thermal processing on its applications, for example, light emitting diodes.[16−18] In this article, we investigated the evolution of CdTe NCs in the PPV:CdTe hybrid film during annealing processing, focusing on the dependence of solar cell performance on various nanoscale phase separation structures, which are influenced by concentration of compositions, annealing temperature, annealing time, and active layer thickness. We propose that a percolation network of CdTe NCs is an efficient phase separation structure for enhancing photo generated current and the performance of PPV:CdTe devices.

Received: October 11, 2011
Revised: December 7, 2011
Published: December 07, 2011

EXPERIMENTAL SECTION

Materials. $NaBH_4$ (99%), tellurium powder (200 mesh, 99.8%), cadmium chloride hemi(pentahydrate) ($CdCl_2 \cdot 2.5H_2O$, 99%), and 2-mercaptoethylamine (MA, 98%) were purchased from Aldrich. *p*-Xylylene dichloride (98%) and tetrahydrothiophene (98%) were purchased from Alfa Aesar. All materials were used as received. Methanol was AR grade, and water was deionized.

Preparation of CdTe NCs and PPV Precursor. MA-stabilized aqueous CdTe NCs were prepared similar to the method described in ref 19. Briefly, 0.28 mL of NaHTe (2/3 M) solution was injected into 12.5 mM N_2-saturated $CdCl_2$ solutions in the presence of MA in the pH range of 5.5−6. The molar ratio of Cd^{2+}/MA/HTe^- was set as 1:2.4:0.2. The resultant precursor solutions were refluxed at 100 °C for 23 min to maintain the growth of CdTe NCs. After that, the NCs solution was centrifugated at a high-speed of 6000 rpm after adding isopropanol to remove superfluous salts and ligands. The precipitated NCs weighed 94 mg and can be redissolved in deionized water to form CdTe NCs aqueous solution with desired concentration.

The PPV precursor was prepared following ref 20. Briefly, the monomer *p*-xylene-bis(tetrahydrothiophenium chloride) was prepared by reaction of dichloro-*p*-xylene (3 g) with 3 mL of tetrahydrothiophene at 50 °C in 40 mL of methanol for 24 h. The product was purified by concentrating the reaction solution and then precipitating the condensed solution in cold acetone (0 °C). The solid was collected by filtration and dried thoroughly in a vacuum oven. After that, 11.6 mL of 0.4 M NaOH solution was added into the *p*-xylene-bis(tetrahydrothiophenium chloride) aqueous solution in 30 min. The reaction continued at 0 °C for 30 min and then was terminated by the addition of 0.4 M HCl aqueous solution to neutralize the reaction solution. Precursor solution then was dialyzed in distilled water for a week. The concentration of the polymer was obtained by evaporating known volumes to dryness and weighing. The solution of PPV precursor in this case was measured to be 4 mg/mL.

Device Fabrication and Characterization. For device preparation, indium tin oxide (ITO) glasses were cleaned ultrasonically in chloroform, acetone, and iso-propyl acohol for 10 min each, and rinsed by deionized water before drying in N_2 flow. After that, a buffer layer of conductive polymer, poly (3,4-ethylene dioxylene thiophene):poly(styrene sulfonic acid) (PEDOT:PSS), was spin coated on the cleaned ITO glass. Active layer film was fabricated by spin-coating the blend solution containing both CdTe NCs and PPV precursor in air condition. When the active layer film is dry, the devices were transferred into a glovebox filled with nitrogen atmosphere (<1 ppm H_2O and <1 ppm O_2) and annealed. The back electrode of 70 nm Al was finally evaporated under high vacuum.

The size and distribution of CdTe NCs in PPV:CdTe film were recorded by the transmission electron microscope (TEM) images and X-ray diffraction (XRD). TEM was conducted using a Hitachi H-800 electron microscope at an acceleration voltage of 200 kV with a CCD camera. XRD data were collected at 298 K on a Bruker SMART-CCD diffractometer. The investigated 2θ range was 20−55° with steps of 0.1°. The surface morphology of PPV:CdTe film was characterized using atomic force microscope (AFM) images. AFM tapping mode measurements were performed on a Nanoscope IIIa scanning probe microscope (Digital Instruments), using a rotated tapping mode etched silicon probe (RTESP) tip. The film thickness was determined using a Dektak150 surface profiler. Current density−voltage ($I-V$) measurement of the devices was conducted on a computer-controlled Keithley2400 source meter measurement system. Air Mass 1.5 global (AM1.5G) 100 mW/cm^2 illumination from a Sciencetech 500-W solar simulator acted as a light source.

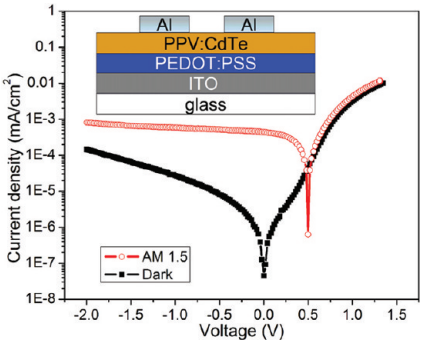

Figure 1. The semilogarithmic plots and the structure (inset) of PPV:CdTe hybrid solar cells.

RESULTS AND DISCUSSION

The structure and performance of PPV:CdTe solar cells fabricated from aqueous solution-processed materials are shown in Figure 1. Although the original materials, both PPV precursor and MA capped CdTe NCs, are soluble in water, the annealed hybrid films are insoluble and infusible due to the essence of rigid-chain conjugated polymer structure. A power PCE above 1.80% has been achieved for this device, which is the highest efficiency for bulk heterojunction solar cells fabricated from aqueous solution ever reported.[12]

As for the solar cells, the processes of photocurrent generation in bulk heterojunction solar cells can be mainly divided into several steps: photon absorption, exciton diffusion, exciton dissociation, charge carrier transport, and collection. The occurrence of photogenerated current is influenced by the micro- and nanoscale phase separation structure of the hybrid film, which plays a key role in the generation and separation of excitons, as well as the transportation and collection of free charges.[21] For the PPV:CdTe blend film, during the annealing treatment, the PPV precursor conducts elimination reaction to drive off the remaining small molecules, such as tetrahydrothiophene, HCl, and water, and thus yields the rigid conjugated polymer chain. Meanwhile, both interfacial and excess ligands on CdTe NCs, which act as a barrier for charge transfer from polymer to NCs and NCs to NCs, are removed. The annealing process thus converts PPV and NC solids from insulators to semiconductors. More interestingly, the CdTe NCs will continuously grow during the annealing process, which greatly changes the phase separation structure of the PPV:CdTe films. Before annealing, the CdTe NCs dispersed even in PPV matrix. During annealing, the NCs grow and form larger nanoclusters, resulting in the percolation network phase separation structure in PPV:CdTe hybrid films. This structure has two prominent features. On one hand, similar to that of the CdTe NCs as made,[19] the annealed CdTe NCs are single crystal with zinc blende structure (Figure S1), which implies that separated charges will transport and be collected more efficiently due to the high carrier mobilities of CdTe crystal.[12] On the other hand, our result confirms that the percolation network of CdTe NCs is effective for excitons generation and separation due to the size and distribution of CdTe in PPV matrix. For the in-depth understanding these two

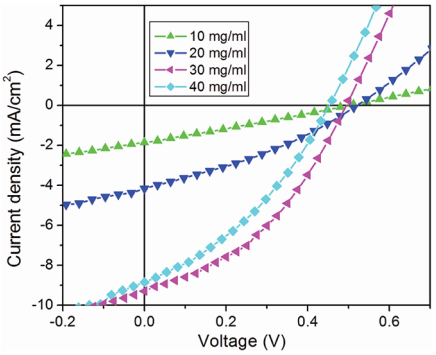

Figure 2. Dependence of J_{sc} of the ITO/PEDOT:PSS/PPV:CdTe/Al device on the concentration of CdTe NCs.

features, the influence of the experimental variables on the device performance is systematically studied.

Effect of Concentration. The performance of solar cells usually shows composition dependence.[22] By mixing the PPV precursor (4 mg/mL) and CdTe NCs (60 mg/mL) together, hybrid films with different composition content were achieved via the spin-coating method. The experimental photocurrent−voltage properties of PPV:CdTe hybrid solar cells as a function of CdTe concentration are presented in Figure 2. When the concentration of CdTe is lower than 30 mg/mL, the short circuit current (J_{sc}) and PCE increase with CdTe concentration. The open circuit voltage (V_{oc}) is found to slightly decrease, which was believed to be due to the change of the inorganic acceptor conduction band (CB). As a function of highest occupied molecular orbital (HOMO) of the polymer and CB of inorganic NCs,[23] the V_{oc} decreased due to the annealing induced growth of CdTe NCs, which move the CB of CdTe NC farther away from vacuum level.[2] The increase of PCE of the hybrid solar cells is mainly due to the difference in J_{sc} and the fill factor (FF). When CdTe is 30 mg/mL, the PCE reached the top value of 1.80%. Further increasing CdTe NCs will lead to a decrease of performance.

To gain insight into the nanostructure within the films, the annealed PPV:CdTe films with different compositional content were investigated using TEM (Figure 3). The solutions used were the same as that for the solar cell devices; however, to clarify the internal structure of PPV:CdTe films, the thicknesses of the films (about 40 nm) were thinner than that of the devices (about 100 nm) by improving the spin-coating rate. By increasing the content of CdTe NCs, the nanoclusters keep on growing. For pure PPV film, no apparent clusters are observed. When concentration of CdTe is 5 mg/mL, isolated spheres/nanoclusters appear with the average diameter of 8.5 nm. Further increasing CdTe NCs content, the nanoclusters become even larger until an average diameter of 25.8 nm (CdTe, 30 mg/mL). Further increasing CdTe content to 40 mg/mL, the nanoclusters connect with each other and form a continuous structure (Figure 3f). The shape of the nanoclusters is spherical or elliptic until they connect with each other and form a continuous structure. We speculate that the growth of CdTe NCs was achieved by the collective motions of smaller NCs or clusters, which make them fuse into larger NCs,[24−26] and the growth mechanism in detail will be discussed in the following. Correlating the device performance and active layer structure, we may confirm that when the highest PCE is achieved, the CdTe showed the percolation network structure; that is, the NCs in

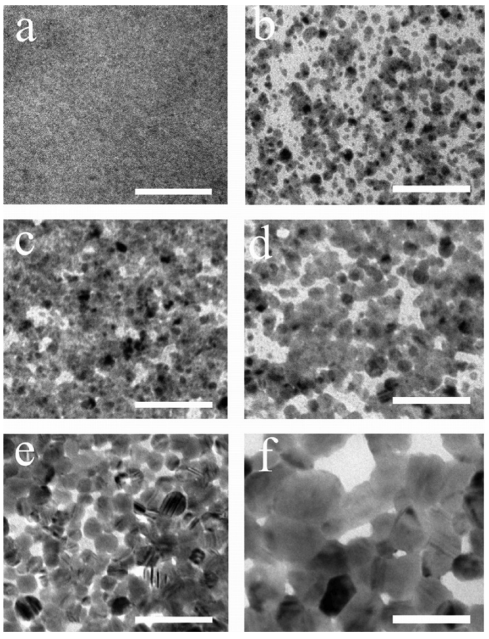

Figure 3. TEM images of PPV:CdTe with different CdTe contents: (a) 0 mg/mL; (b) 5 mg/mL; (c) 10 mg/mL; (d) 20 mg/mL; (e) 30 mg/mL; (f) 40 mg/mL. The films were annealed at 320 °C for 60 min. Scale bar: 100 nm.

the active layer aggregate together and form regions of densely packed NCs surrounded by regions of polymer. Meanwhile, the PPV layer among CdTe nanoclusters is in the range of 6−15 nm. It has been reported that singlet excitons in PPV can diffuse over a length of 12 nm in thin films consisting of PPV;[27,28] the phase separation structure of PPV:CdTe film is therefore believed favored for the diffusion and separation of excitons, thus improving photogenerated current. When the content of CdTe is too low, the formation and separation of excitons is inefficient. Otherwise, when CdTe is higher above 30 mg/mL, the overgrowth of CdTe nanocluster will unavoidably decrease the interface between PPV and CdTe, decreasing the photocurrent and PCE of PPV:CdTe solar cells accordingly.

The annealing-induced change of the structure of PPV:CdTe hybrid film is different from that of polymer/fullerene solar cells and that of polymer/NCs solar cells fabricated from organic solvents. For polymer/fullerene solar cells, for example, the poly(3-hexylthiophene)(P3HT)/[6,6]-phenyl-C61-butyric acid methyl ester(PCBM) system, the P3HT will realize crystallization via self-assembly during the annealing process,[29] and the aggregation and phase separation of PCBM happens.[22] The size of PCBM cluster is up to several hundred nanometers. For polymer/CdSe NCs solar cells fabricated from organic solvents, the phase separation structure of the polymer and the CdSe NCs was observed to be influenced by the size of NCs; the PCEs of devices were once only about 0.1%.[30] This was attributed to an inefficient electron transport via hopping from NCs to NCs. The substantial improvement in the hybrid solar cells performance was achieved by synthesizing CdSe NCs with various morphologies and structures, or by utilizing of mixture of multiple solvents in hybrid solar cells.[31] Elongated nanorods[1] and NCs with tetrapods or hyperbranched[32] structure exhibited improved photo current and PCE due to the improved electron transport properties, and using the mixture of solvents might lead to a more favorable donor−acceptor phase separation structure.

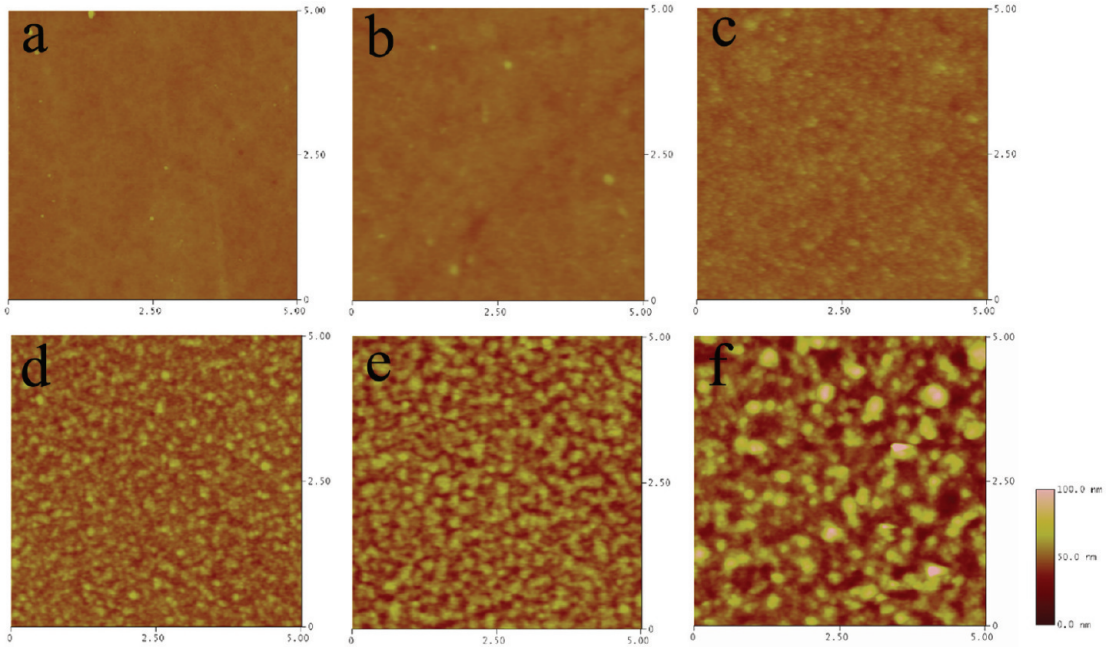

Figure 4. AFM images of PPV:CdTe films with different CdTe contents: (a) 0 mg/mL; (b) 5 mg/mL; (c) 10 mg/mL; (d) 20 mg/mL; (e) 30 mg/mL; (f) 40 mg/mL. The films were annealed at 320 °C for 60 min.

Corresponding to the composition change, the surface nanoscale morphology of the active layer of the solar cells was studied with tapping mode AFM. Figure 4 presents the surface morphology of PPV:CdTe films with various compositional content. It is clear that with the increase of CdTe content, the surface of the film becomes rougher, indicating the growth of CdTe nanoclusters. For pure PPV film (CdTe, 0 mg/mL), the root-mean-square (rms) roughness is 0.97 nm. For PPV:CdTe flms, the rms value increase from 1.69 nm (CdTe, 5 mg/mL) to 7.58 nm (CdTe, 40 mg/mL). The surface features show that the average size of CdTe nanoclusters increases from 38 nm (CdTe, 5 mg/mL) to above 300 nm (CdTe, 40 mg/mL). The increase of rms reflects the growth of CdTe NCs in film and is in accordance with the TEM results.

The growth of NCs in polymer media relates to both the growth kinetics of NCs themselves and the nature of the polymers.[33−35] Although the transition of PPV precursor to PPV has been systematically investigated in previous studies,[14,36−38] the growth of NCs in PPV matrix is still less reported. The growth of CdTe in PPV is through aggregation-limited and/or diffusion-limited processes, which can be analyzed following the Smoluchowski model:

$$\frac{C}{1 + \mu_1\mu_3} = \frac{B(S-1)(v^+)^{-1}}{\frac{2kT}{3\mu}(1 + \mu_1\mu_3)N} \quad (1)$$

where B was the proportionality coefficient in the equation for the condensation rate, S was the supersaturation, v^+ was the mean particle volume, k was Boltzmann's constant, μ and T were the viscosity and temperature of growth medium, and N was the total number concentration of particles. According to this equation, the relative contributions of dynamic coalescence or Ostwald ripening (OR) growth can be confined by calculating μ_1 and μ_3,[26] where $\mu_1 = R_3/R_h, \mu_3 = R_1/R_3$, and that $R_1 = \Sigma R_i/n$, $R_3 = (\Sigma R_i^3/n)^{1/3}$, $R_h = n/\Sigma(1/R_i)$. In this case, the $1 < \mu_1 < 1.25$ and $0.905 < \mu_3 < 1$, demonstrating that the growth of CdTe NCs was achieved by a combination of dynamic coalescence and OR process. Moreover, during the initial stage, growth occurs by simultaneous OR and coalescence, and that coalescence becomes more significant with annealing time extending (see Supporting Information, Table 1).

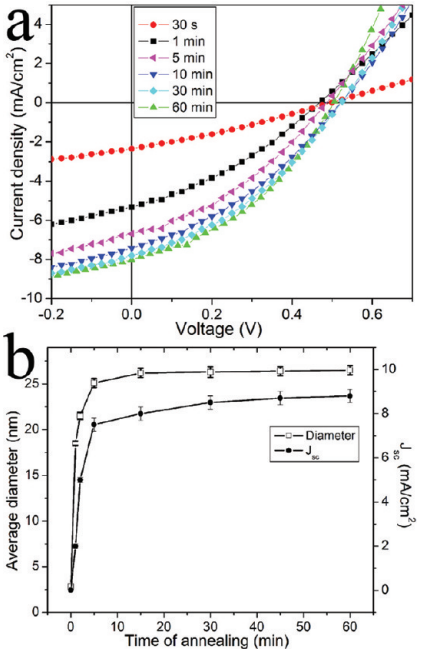

Figure 5. (a) $I-V$ and (b) dependence of short-circuit current (J_{sc}) and average diameter of CdTe NCs on annealing time. Annealing temperature: 320 °C. CdTe: 30 mg/mL.

Effect of Annealing Temperature and Time. The conversion of PPV precursor to PPV and deprival of ligands on CdTe NCs are necessary for enhancing the photovoltaic effect. PPV precursor allows the conversion to occur in the temperature

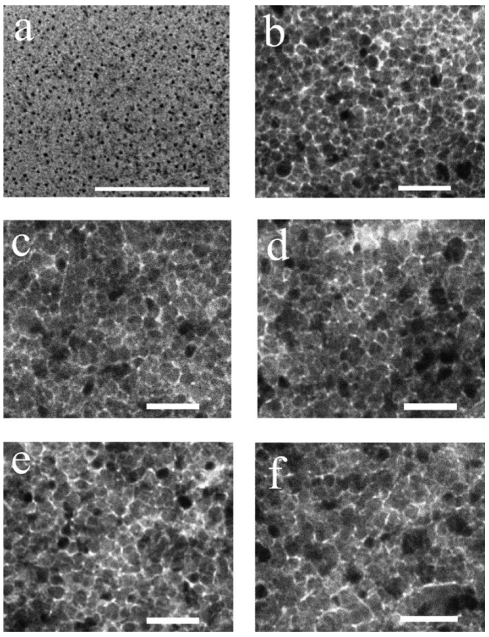

Figure 6. TEM images of PPV:CdTe films after annealing for (a) 0 min; (b) 30 s; (c) 1 min; (d) 2.5 min; (e) 5 min; (f) 60 min. Annealing temperature: 320 °C. CdTe: (a) 5 mg/mL, (b)−(f) 30 mg/mL. Scale bar: 100 nm.

range of 80−400 °C under vacuum.[39,40] Higher temperature will improve the conversion rate. For CdTe NCs, thermogravimetric analysis (TGA) characterization indicates that the elimination reaction starts at 240 °C, and the deprival rate reaches a peak at 300 °C.[12]

The photocurrent−voltage properties of PPV:CdTe hybrid solar cells as a function of annealing time are shown in Figure 5. The J_{sc} values increase quickly in the first 5 min, and then become gradually stable after that. This result indicates that most interfacial ligands on CdTe NCs and most small molecules on PPV were deprived of in 5 min. The apparent color of hybrid films turned from wine to dark yellow within 1 min, implying that the CdTe NCs grow quickly during the time. To investigate the effect of annealing time on size and phase separation structure of the PPV:CdTe films, samples annealed for different time are compared in TEM (Figure 6). It is found that the CdTe nanoclusters increase immediately after annealing at 320 °C, demonstrating the fast dynamic process of NCs growth. The original average size of CdTe is 2.8 nm, which reaches 17.2 nm after annealing for 30 s. After that, the average size of CdTe clusters increase slowly to 26.5 nm after 60 min. The hybrid film with full-grown NCs shows better performance, leading from the reduced charge loss as the charge transfer occurs in between NCs. Further increase the annealing temperature over 320 °C cannot enhance the performance, because once CdTe clusters reach a specific size, the growth will stop, and hence the morphology evolution terminates. Moreover, the morphological stability of the hybrid film is high enough against the corrosion of water and oxygen in the air. By comparing the difference of time between the increase of J_{sc} and the growth of CdTe NCs, we believe that the PPV precursor needs more time to convert than does CdTe. As a result, the flexible polymer molecular chains permit the CdTe nanoclusters to come closer and fuse into larger NCs. Here, it is worth mentioning that the mechanism is closely

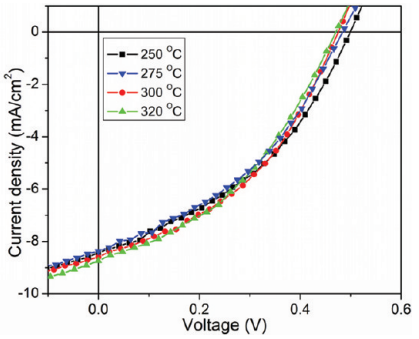

Figure 7. Dependence of solar cells performance on annealing temperature. CdTe: 30 mg/mL. Annealing time: 15 min.

connected with the rapid desorption of the MA ligands.[25] The annealing temperature is much higher than that needed for ligands removal, confirming that the CdTe cores are able to fuse immediately once they approach each other close enough.[41,42] However, the increase of photocurrent is determined by both growth of CdTe nanoclusters and the conversion of PPV precursor. The slight inconsistency of the increasing time between photocurrent and average diameter of CdTe NCs may lie in the low conversion rate of PPV material. The growth of CdTe NCs needs several minutes, while conversion of PPV precursor needs several hours.[14] The crystallinity and growth of CdTe nanoclusters after the annealing treatment were illustrated by X-ray diffraction (XRD), as shown in Figure S1. The XRD spectra clearly exhibit peaks at 24.2°, 39.8°, and 47.1°, which correspond to the (111), (220), and (311) faces of the CdTe crystals. The result indicates that annealing treatment does not change the crystallinity of CdTe crystals. The size of CdTe nanoclusters can also be estimated by the XRD data. According to the Scherrer formula, the size of CdTe nanoclusters increases with the prolonging of annealing time. The increase in size is consistent with the TEM results, as shown in Table 2, Supporting Information.

According to the time−temperature equivalence principle, prolonging the annealing time works the same as increasing the annealing temperature. The dependence of solar cells performance on annealing temperature was also investigated, and the results were shown in Figure 7. When T was below 240 °C (the CdTe NCs start to grow when temperature is above 110 °C[35]), although the NCs increase rapidly, no apparent photocurrent was observed. When T was 250 °C, the photovoltaic effect was found after 10 min. This comparison indicates that the ligands deprival occurs between 240 and 250 °C, which is consistent with the TGA result.[12] Further increasing the annealing temperature, the J_{sc} is nearly constant. What is more, the V_{oc} is found to decrease with the increase of annealing temperature, which was due to the decrease of CB of CdTe caused by extended coalescence as mentioned before. Figure 8 shows the TEM images of PPV:CdTe film annealed under different temperature, which indicates that the growth of CdTe nanoclusters is similar to that enduring different annealing time. The XRD spectra (Figure S2) indicate the CdTe NCs grow faster under higher the annealing temperature. The dependence of CdTe evolution on annealing temperature can be explained via free volume theory that a higher annealing temperature enhanced the fractional free volume of the polymer media and provided more spaces for the

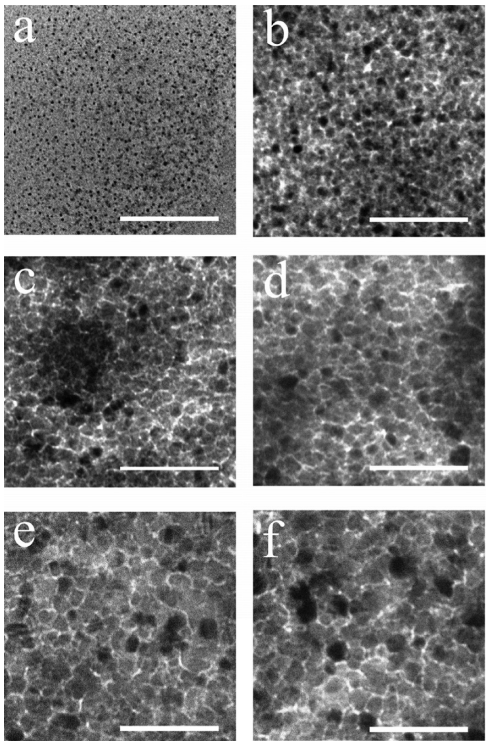

Figure 8. TEM images of PPV:CdTe films before (a) and after annealing at (b) 200 °C; (c) 240 °C; (d) 250 °C; (e) 280 °C; (f) 320 °C for 10 min. CdTe: (a) 5 mg/mL, (b)−(f) 30 mg/mL. Scale bar: 100 nm.

motion of NCs and polymer chains. Consequently, the aggregation and fusion of NCs were favored, leading to a higher growth rate of NCs (Table 3, Supporting Information).

Effect of Active Layer Thickness. Besides the compositional content, annealing time, and annealing temperature, the performances of solar cells are still closely affected by the active layer thickness. Under illumination, light is absorbed and charges are generated throughout the bulk. The generation rate G, the number of charges generated inside a device of area A per second, is then given by the number of photons absorbed per second as follows:

$$G = \nu_{cs}\varphi_{photon}A(1 - e^{-\alpha d}) \quad (2)$$

which is a function of the incident photon flux φ_{photon}, giving the number of incident photons per second and area, the absorption coefficient α, the thickness d of the layer, and the probability for the separation ν_{cs} of the generated excitons into free charge carriers.[43] The equation means that one could increase active layer thickness d to improve the generation of charges until a constant photogenerated current is achieved.

Conjugated polymers typically have a high absorption coefficient above 10^5 cm^{-1}, and therefore a thin layer of active material with a thickness of 100−300 nm is enough for sufficient light harvesting.[2,27] In this case, when the active layer is in the range of 0−100 nm, the relationship between the J_{sc} and active layer thickness is shown in Figure 9. It is found there is a linear relationship between the photocurrent (i.e., J_{sc}) of PPV:CdTe solar cells and the thickness of active layer. The highest J_{sc} was achieved when the active layer is around 100 nm thick. This result obeys the Beer−Lambert law. Under this consideration, a thicker active layer is able to absorb more photons and create more excitons,and thus a higher photogenerated current is expected if

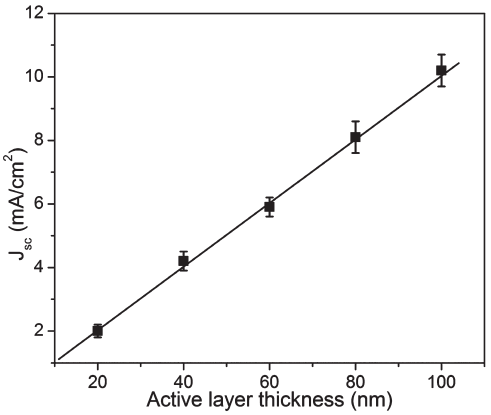

Figure 9. Relationship between the short-circuit current and the thickness of active layer for PPV:CdTe solar cells. CdTe: 30 mg/mL. Annealing time: 15 min.

we can increase the active layer thickness. However, our experiments show that a thicker active layer will unavoidably increase the series resistance of the device, and thus lead to a decrease of photocurrent and cell performance.

For PPV:CdTe film, the densely packed PPV:CdTe phase separation structure confirms that the distance between donor/acceptor interfaces and the photoexcitation sites are optimized to be within the range of exciton diffusion length in the bulk-heterojunction device structure, so the exciton dissociation is efficient. The charge transport and collection will be enhanced in a thick active layer due to the high carrier mobilities of PPV and CdTe crystal.[12] What is more, it is worth pointing out that the viscosity of PPV:CdTe blending solution is key to the thickness of the resulting film. PPV with a high molecular weight and a high concentration has a high viscosity and is prone to produce a thicker active layer film. Although the viscosity of PPV is doomed to decrease after incorporating CdTe solution, a solution with a high concentration of CdTe NCs is still preferred, with the expense of lifetime and stability.

CONCLUSION

The annealing-induced growth of CdTe NCs in PPV:CdTe hybrid solar cell, fabricated from aqueous solution processed materials, was investigated to reveal the dependence of performance on nanoscale phase separation structure. Mainly via the dynamic coalescence mechanism, the growth of CdTe NCs in PPV matrix shows dependence on CdTe concentration, annealing temperature, annealing time, and active layer thickness. The best performance of hybrid solar cells was achieved when CdTe was 30 mg/mL, the annealing temperature was above 250 °C, with the active layer thickness of 100 nm. Correspondingly, a percolation network phase separation structure was observed in the active layer. The result shows the specificity of nanoscale phase separation structure of solar cells processed from aqueous solution.

ASSOCIATED CONTENT

Supporting Information. XRD characterization of PPV:CdTe hybrid films annealed under different temperatures and for different times. This material is available free of charge via the Internet at http://pubs.acs.org.

AUTHOR INFORMATION

Corresponding Author
*Tel.: +86 431 85168478. Fax: +86 431 85193423. E-mail: byangchem@jlu.edu.cn.

ACKNOWLEDGMENT

This project was supported by the National Natural Science Foundation of China (50973039, 20921003, and 91123031) and the National Basic Research Development Program of China (2012CB933802).

REFERENCES

(1) Huynh, W. U.; Dittmer, J. J.; Alivisatos, A. P. *Science* **2002**, *295*, 2425–2427.
(2) Xu, T.; Qiao, Q. *Energy Environ. Sci.* **2011**, *4*, 2700–2720.
(3) Zhou, Y.; Eck, M.; Kruger, M. *Energy Environ Sci.* **2010**, *3*, 1851–1864.
(4) Hoppe, H.; Niggemann, M.; Winder, C.; Kraut, J.; Hiesgen, R.; Hinsch, A.; Meissner, D.; Sariciftci, N. S. *Adv. Funct. Mater.* **2004**, *14*, 1005–1011.
(5) Beek, W. J. E.; Janssen, R. A. J. *Adv. Funct. Mater.* **2002**, *12*, 519–525.
(6) Beek, W. J. E.; Wienk, M. M.; Janssen, R. A. J. *Adv. Mater.* **2004**, *16*, 1009–1013.
(7) Gunes, S.; Fritz, K. P.; Neugebauer, H.; Sariciftci, N. S.; Kumar, S.; Scholes, G. D. *Sol. Energy Mater. Sol. Cells* **2007**, *91*, 420–423.
(8) Schaller, R. D.; Klimov, V. I. *Phys. Rev. Lett.* **2004**, *92*, 186601.
(9) Andersen, T. R.; Larsen-Olsen, T. T.; Andreasen, B.; Böttiger, A. P. L.; Carlé, J. E.; Helgesen, M.; Bundgaard, E.; Norrman, K.; Andreasen, J. W.; Jørgensen, M.; Krebs, F. C. *ACS Nano* **2011**, *5*, 4188–4196.
(10) Espinosa, N.; García-Valverde, R.; Urbina, A.; Krebs, F. C. *Sol. Energy Mater. Sol. Cells* **2011**, *95*, 1293–1302.
(11) Søndergaard, R.; Helgesen, M.; Jørgensen, M.; Krebs, F. C. *Adv. Energy Mater.* **2011**, *1*, 68–71.
(12) Yu, W.; Zhang, H.; Fan, Z.; Zhang, J.; Wei, H.; Zhou, D.; Xu, B.; Li, F.; Tian, W.; Yang, B. *Energy Environ. Sci.* **2011**, *4*, 2831–2834.
(13) Garay, R. O.; Sarimbalis, M. N.; Hernández, S. A.; Montani, R. S. *Macromolecules* **2000**, *33*, 4398–4402.
(14) Shah, H. V.; Arbuckle, G. A. *Macromolecules* **1999**, *32*, 1413–1423.
(15) Herold, M.; Gmeiner, J.; Schwoerer, M. *Polym. Adv. Technol.* **1999**, *10*, 251–258.
(16) Burroughes, J. H.; Bradley, D. D. C.; Brown, A. R.; Marks, R. N.; Mackay, K.; Friend, R. H.; Burns, P. L.; Holmes, A. B. *Nature* **1990**, *347*, 539–541.
(17) Gustafsson, G.; Cao, Y.; Treacy, G. M.; Klavetter, F.; Colaneri, N.; Heeger, A. J. *Nature* **1992**, *357*, 477–479.
(18) Zheng, M.; Sarker, A. M.; Gurel, E. E.; Lahti, P. M.; Karasz, F. E. *Macromolecules* **2000**, *33*, 7426–7430.
(19) Zhang, H.; Wang, L. P.; Xiong, H. M.; Hu, L. H.; Yang, B.; Li, W. *Adv. Mater.* **2003**, *15*, 1712–1715.
(20) Jin, S. H.; Jang, M. S.; Suh, H. S.; Cho, H. N.; Lee, J. H.; Gal, Y. S. *Chem. Mater.* **2002**, *14*, 643–665.
(21) Peumans, P.; Uchida, S.; Forrest, S. R. *Nature* **2003**, *425*, 158–162.
(22) Mihailetchi, V. D.; Koster, L. J. A.; Blom, P. W. M.; Melzer, C.; de Boer, B.; van Duren, J. K. J.; Janssen, R. A. J. *Adv. Funct. Mater.* **2005**, *15*, 795–801.
(23) Ishwara, T.; Bradley, D. D. C.; Nelson, J.; Ravirajan, P.; Vanseveren, I.; Cleij, T.; Vanderzande, D.; Lutsen, L.; Tierney, S.; Heeney, M.; McCulloch, I. *Appl. Phys. Lett.* **2008**, *92*, 053308.
(24) Piepenbrock, M.-O. M.; Stirner, T.; O'Neill, M.; Kelly, S. M. *J. Am. Chem. Soc.* **2007**, *129*, 7674–7679.
(25) Meli, L.; Green, P. F. *ACS Nano* **2008**, *2*, 1305–1312.
(26) Tang, Y.; Zhang, H.; Fan, Z.; Li, M.; Han, J.; Dong, F.; Yang, B. *Phys. Chem. Chem. Phys.* **2010**, *12*, 11843–11849.
(27) Carsten, D.; Vladimir, D. *Rep. Prog. Phys.* **2010**, *73*, 096401.
(28) Nguyen, T.-Q.; Schwartz, B. J.; Schaller, R. D.; Johnson, J. C.; Lee, L. F.; Haber, L. H.; Saykally, R. J. *J. Phys. Chem. B* **2001**, *105*, 5153–5160.
(29) Ma, W. L.; Yang, C. Y.; Gong, X.; Lee, K.; Heeger, A. J. *Adv. Funct. Mater.* **2005**, *15*, 1617–1622.
(30) Greenham, N. C.; Peng, X.; Alivisatos, A. P. *Phys. Rev. B* **1996**, *54*, 17628–17637.
(31) Dayal, S.; Kopidakis, N.; Olson, D. C.; Ginley, D. S.; Rumbles, G. *Nano Lett.* **2010**, *10*, 239–242.
(32) Sun, B.; Marx, E.; Greenham, N. C. *Nano Lett.* **2003**, *3*, 961–963.
(33) Bockstaller, M. R.; Mickiewicz, R. A.; Thomas, E. L. *Adv. Mater.* **2005**, *17*, 1331–1349.
(34) Dan, N.; Zubris, M.; Tannenbaum, R. *Macromolecules* **2005**, *38*, 9243–9250.
(35) Zhang, H.; Tang, Y.; Zhang, J.; Li, M.; Yao, X.; Li, X.; Yang, B. *Soft Matter* **2009**, *5*, 4113–4117.
(36) Adriaensens, P.; Roex, H.; Vanderzande, D.; Gelan, J. *Polymer* **2005**, *46*, 1759–1765.
(37) Wery, J.; Dulieu, B.; Baitoul, M.; Paniez, P.; Froyer, G.; Lefrant, S. *Synth. Met.* **1999**, *101*, 194–195.
(38) Seoul, C.; Kang, J. I.; Mah, S. I.; Lee, C. H. *Synth. Met.* **1999**, *99*, 35–43.
(39) Garay, R. O.; Baier, U.; Bubeck, C.; Müllen, K. *Adv. Mater.* **1993**, *5*, 561–564.
(40) Kraft, A.; Grimsdale, A. C.; Holmes, A. B. *Angew. Chem. Int. Ed.* **1998**, *37*, 402–428.
(41) Pich, J.; Friedlander, S. K.; Lai, F. S. *J. Aerosol Sci.* **1970**, *1*, 115–126.
(42) Talapin, D. V.; Rogach, A. L.; Shevchenko, E. V.; Kornowski, A.; Haase, M.; Weller, H. *J. Am. Chem. Soc.* **2002**, *124*, 5782–5790.
(43) Waldauf, C.; Scharber, M. C.; Schilinsky, P.; Hauch, J. A.; Brabec, C. J. *J. Appl. Phys.* **2006**, *99*, 104503.